ISBN: 978-3-95450-262-2 ISSN: 2673-5350 doi: 10.18429/JACoW-IBIC2025-TUPMO32

WIDE RANGE LOW COST DIGITAL RF PHASE SHIFTER

K. Zenker*, U. Lehnert, A. E. Rivera Osorio, R. Steinbrück, M. Kuntzsch
Institute of Radiation Physics, Helmholtz-Zentrum Dresden-Rossendorf, Dresden, Germany

Abstract

Shifting RF phases is a common task in particular at particle accelerators. At the ELBE Center for High-Power Radiation Sources we use the phase shifter to shift the phase of the superconducting RF gun laser with respect to the accelerator cavity RF field and for delay compensation in general. The phase shifter presented in this contribution consists of a custom board, that includes a high-performance quadrature modulator, voltage regulators and an 16-bit digital-to-analogue converter that offers an I2C interface. The quadrature modulator is specified to work in the frequency range between 50 MHz and a 6 GHz. The board is combined with commercial off-the-shelf products to provide a software interface, which in our case is implemented as OPC UA interface. All components are integrated to a compact RF tight housing. We present amplitude and phase noise measurements and amplitude stability measurements at selected frequencies in the range between 78 MHz and 1.3 GHz.

INTRODUCTION

At particle accelerators the ability to shift the phase of a radio frequency (RF) signal is a common task. Different commercially available phase shifters exist. They make use of different approaches of shifting the RF phase, e.g. in case of mechanical phase shifters the length of an RF guide is manipulated, they cover different frequency ranges and they provide different interfaces, such as knobs (mechanical), input voltage (analog) or digital interfaces. In addition, not all phase shifter are able to shift the RF phase by full 360°. However, none of the commercial available solutions covered our requirements at ELBE Center for High-Power Radiation Sources [1] listed in Table 1.

Table 1: Phase Shifter Requirements at ELBE

Frequency range	78 MHz to 3900 MHz
Input level	−5 dBm to 12 dBm
Phase noise jitter at 1.3 GHz	≤ 10 fs
Phase stability (24h)	0.1°
Amplitude stability (24h)	≤ 0.1 dB
Phase range	360°
Supply voltage	12 V
Interface	digital

The phase shifter presented here was designed to fulfill these requirements. It is based on a quadrature modulator introduced in the following.

* k.zenker@hzdr.de

PHASE SHIFTER BOARD

The main component of the phase shifter board (PSB) is the low-noise direct quadrature modulator TRF370417 from Texas Instruments [2]. It is implemented as a double balanced mixer. Figure 1 shows an overview of the phase shifter including a picture of the 7 cm × 5.5 cm 2-layer printed circuit board that uses a ground plane in the RF section and ground vias surrounding the RF lines. The in-phase positive

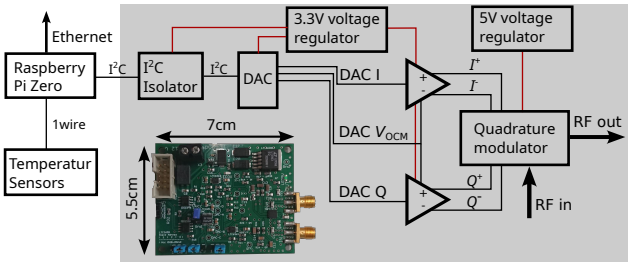

Figure 1: Phase shifter block diagram. The gray box indicates components that are part of the printed circuit board. In the addition a picture of the fully equipped printed circuit board is shown.

and negative inputs (I^+, I^-) as well as the quadrature-phase positive and negative input signals (Q^+, Q^-) are generated using a differential operational amplifier (LTC6363 [3]). A digital-to-analog converter [4] (DAC) is used to generate the differential operational amplifier input signals. It is also used to generate the output common mode voltage of the differential operational amplifier that is defined as

$$V_{\mathrm{OCM}} = \frac{V_{\mathrm{out}}^{+} + V_{\mathrm{out}}^{-}}{2}.$$

For best linearity of the quadrature modulator V_{OCM} is set to 1.7 V [3] for all measurements presented below. The DAC has 16-bit resolution and provides an I^{2}C interface. For ground isolation, high voltage protection and to prevent noise currents from entering the local ground a bidirectional I^{2}C isolator ISO1541 [5] is added to the board. The board is configured such that the maximum baseband voltage - i.e. for the in-phase voltage $V_{\mathrm{BB},I} = |I^+ - I^-|$ - is 1 V for the maximum DAC setting. The quadrature modulator output power level in dependence of the baseband voltage is shown in Fig. 2a. Figure 2b shows the measured output power P_{out} as a function of the RF frequency at maximum V_{BB} in the range of 50 MHz to 5 GHz.

The quadrature modulator is powered by a 12 V low noise voltage regulator LT1761 [6], whereas the DAC, I^{2}C isolator and the differential operational operators are power by a 3.3 V low noise voltage regulator LT1963 [7].

ISBN: 978-3-95450-262-2 ISSN: 2673-5350 doi: 10.18429/JACoW-IBIC2025-TUPMO32

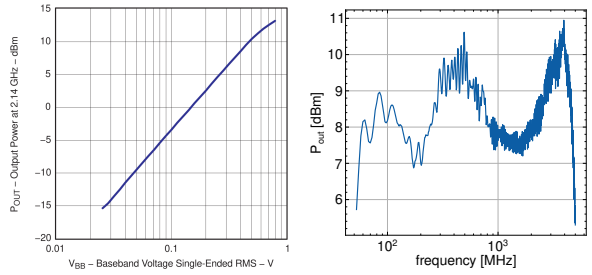

(a) P_{out} in dependence of the baseband voltage V_{BB} [2].

(b) P_{out} in dependence of the RF frequency at $P_{\text{in}} = 5\,\text{dBm}$ and maximum V_{BB}.

Figure 2: Characterization of the quadrature modulator.

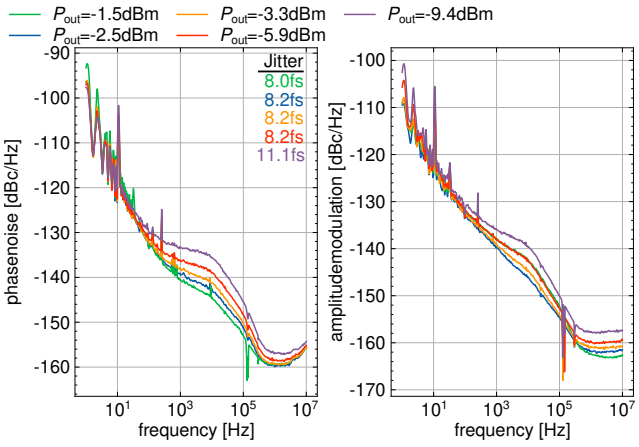

Figure 3: PN (left) and AM (right) at 1.3 GHz and $P_{in} = 5\,\text{dBm}$. The jitter is integrated from 1 Hz to 10 MHz.

Phase Shifter Board Characterization

Noise measurements were performed using a Signal Source Analyser [8] (SSA) measuring amplitude modulation (AM) and phase noise (PN). The internal signal source was used to perform additive noise measurements. Figure 3 shows AM and PN for different P_{out} measured at an RF frequency of 1.3 GHz. As can be seen the noise is reduced with higher P_{out}. However this is a minor effect and e.g. the jitter is only reduced by 0.9 fs in the range 1 Hz to 10 MHz. Figure 4 shows AM and PN for different RF frequencies and integrated measurements are summarized in Table 2. As can be seen, PN and AM is similar for all frequencies except for 78 MHz, which is close to the lower operation frequency of the TRF370417. Comparing the noise between $P_{\text{in}} = 5\,\text{dBm}$ and $P_{\text{in}} = 0\,\text{dBm}$ resulted in a jitter reduction of 2 fs and a reduction of AM of 0.0017 %. The statistical uncertainties for all measurements are below 0.05 m° for PN and below 0.0005 % for AM.

Output Calibration

P_{out} depends on P_{in}, the phase and V_{BB} set using the DAC. We measured P_{out} in dependence of all parameters as shown for 1.3 GHz in Fig. 5. Here scale is the scaling factor of V_{BB} with respect to the maximum value. For a fixed phase and

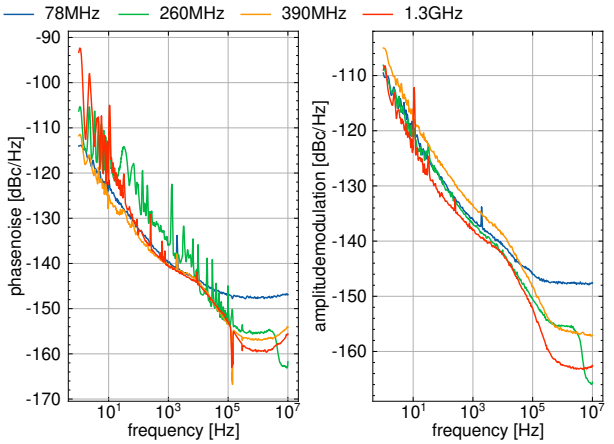

Figure 4: PN (left) and AM (right) for different RF frequencies at $P_{\text{out}} = -2.5\,\text{dBm}$ and $P_{\text{in}} = 5\,\text{dBm}$. The jitter is given in Table 2.

Table 2: Additive noise for different RF frequencies. The noise is integrated from 1 Hz to 10 MHz and 10 Hz to 1 MHz for numbers is brackets. The output power was set to $P_{\text{out}} = -2.5\,\text{dBm}$ and the input power was set to $P_{\text{in}} = 5\,\text{dBm}$.

Frequency	Amplitude Noise [%]	Phase Noise [m°]	Jitter [fs]
1.3 GHz	0.0041 (0.0027)	3.8 (1.5)	8.2 (3.3)
390 MHz	0.0077 (0.0045)	4.4 (1.5)	31.4 (11.2)
260 MHz	0.0057 (0.0036)	3.7 (2.3)	40.3 (24.8)
78 MHz	0.0188 (0.0066)	11.2 (3.5)	401.6 (126.3)

P_{in} the RF output voltage scales linear with V_{BB} (see bottom figures of Fig. 5). Using an P_{in} and phase dependent V_{BB} the phase shifter was calibrated, which ensures a constant RF output voltage. Figure 6 shows that the residual P_{out} deviation from the mean output power is less than ±0.02 dBm after calibration and thus P_{out} can be considered independent of P_{in} and phase after calibration.

Phase Shifter Board Integration

The PSB introduced above was integrated into a 11 cm × 17 cm × 3 cm RF tight housing, which includes SMA RF feedthroughs for RF input and output as well as an RJ45 feedthrough used to connect an internal single board computer to Ethernet. In principle, it would be possible to configure the PSB using a micro controller, but we have chosen a single board computer running a linux based operating system because it offers more flexibility and allows to use commonly available software. The internal single board computer is a Raspberry Pi Zero [9] with an commercial Ethernet hat module. It is responsible of configuring the phase shifter module via I^2C and of reading temperature sensors (DS18B20) via the 1wire protocol [10]. The software framework ChimeraTK [11, 12] is used to implement an OPC UA [13] server utilizing the OPC UA Adapter [14] included in the framework. An OPC UA client based on LabView [15] is used to create a graphical user interface

ISBN: 978-3-95450-262-2 ISSN: 2673-5350 doi: 10.18429/JACoW-IBIC2025-TUPMO32

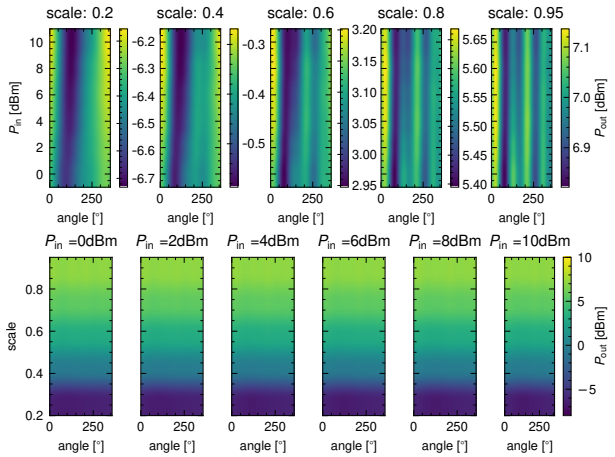

Figure 5: Calibration data for 1.3 GHz. For the upper plots the same P_{in} scale applies for all plots and it is only shown on the left. The labels shown on the right-hand side of each upper plot correspond to the P_{out} scale. For the lower plots, the scale scale shown on the left-hand side and the P_{out} scale shown on the right-hand side apply for all plots.

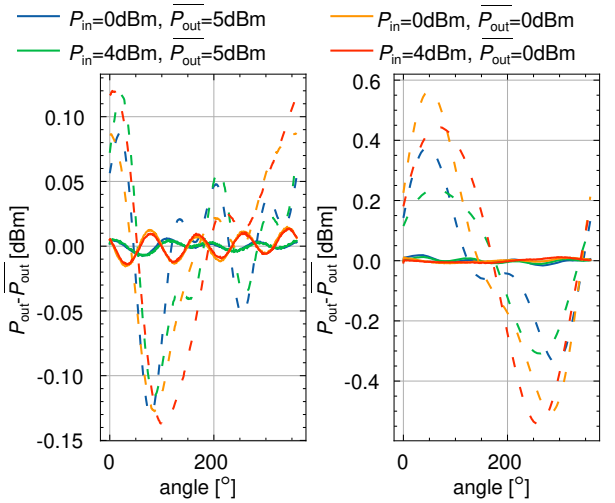

Figure 6: Uncalibrated (dashed lines) and calibrated (solid lines) RF output power deviations for two different RF input and output levels. Left plot shows 1.3 GHz data and right plot shows 390 MHz data.

and a Telegraf [16] client is used to archive the phase shifter data to an Influx data base [16]. Also the integration into the ELBE WinCC [17] control system is done via OPC UA. The power consumption of the PSB is 3.1 W at 12 V and can be reduced lowering the supply voltage. At the minimum supply voltage of 5 V the power consumption is 1.2 W. In addition, the power consumption by the Raspberry Pi Zero is about 1.2 W. We measured the temperature inside the housing, at it reached equilibrium within 2 h at an environmental temperature of 25 °C. In a long term measurement (see Fig. 7) P_{out} and the phase were stable withing the limits defined in Table 1. The maximum temperature of about 60 °C (see Fig. 7) is within the specs of all components of the PSB.

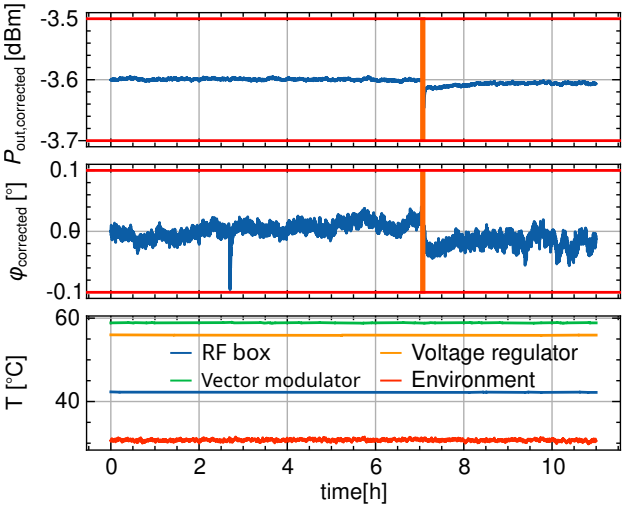

Figure 7: P_{out} (top) and phase (center) of the PSB in a long term measurement at 1.3 GHz. Both are corrected for reference drifts. Red lines indicate the limits from Table 1. Bottom plot shows measured temperatures. At about 7 h the reference was off for a short amount of time (orange box).

APPLICATION AT ELBE

At ELBE we plan to use the phase shifter presented above to implement a feedback loop that stabilizes the phase Φ_{laser} of the laser with respect to the RF phase of the SRF gun [18]. The main effect of changing Φ_{laser} is an energy change of the electron bunch, because the electron released from the cathode by the laser experience a different RF field strength. At ELBE a energy dispersive section (dog leg) is used in front of the first accelerator module. A beam position monitor in this section is used to monitor position and energy changes respectively. This is the feedback loops input and the phase shifter is the control element in the loop that shifts the SRF guns laser phase. Since the laser phase drifts at ELBE happen on an hour time scale implementing the control loop in software will be sufficient in our case.

Furthermore, thanks to the low noise contribution of the phase shifter it is used in the ELBE synchronization system to set amplitude and phase in the pulse picking of the master oscillator replacing commercial components with higher noise contribution.

CONCLUSION

A wide range phase shifter based on a low-noise direct quadrature modulator was presented. PN and AM integrated from 10 Hz to 1 MHz are below 4 m° and 0.007 %. This was measured for ELBE relevant RF frequencies between 78 MHz and 1.3 GHz. The dependency of the RF output power was characterized in dependence of the input power, phase and the modulators baseband voltage. It was shown that after calibration the output power is stable within ±0.2 dBm. The long term stability of the RF output power and phase was demonstrated. Finally, we have shown two different applications of the phase shifter at ELBE.

ISBN: 978-3-95450-262-2 ISSN: 2673-5350 doi: 10.18429/JACoW-IBIC2025-TUPMO32

REFERENCES

[1] P. Michel, "ELBE center for high-power radiation sources", *J. Large-Scale Res. Facil.*, vol. 2, no. A39, 2016. doi:10.17815/jlsrf-2-58

[2] *TRF370417 50-MHz to 6-GHz Quadrature Modulator*, Texas Instruments, Nov. 2015. https://www.ti.com/product/TRF370417

[3] *Precision, Low Power Rail-to-Rail Output Differential Op Amp*, Linear Technology, Nov. 2016. www.linear.com/LTC6363

[4] *Quad I2C 16-/12-Bit Rail-to-Rail DACs with 10ppm/°C Max Reference*, Linear Technology, Jul. 2010. www.linear.com/LTC2655

[5] *ISO154x Low-Power Bidirectional I2C Isolators*, Texas Instruments, Jun. 2015. https://www.ti.com/product/ISO1541

[6] *100mA, Low Noise, LDO Micropower Regulators in TSOT-23*, Linear Technology, May 2010. www.linear.com/LT1761

[7] *1.5A, Low Noise, Fast Transient Response LDO Regulators*, Linear Technology, Jul. 2010. www.linear.com/LTC2655

[8] G. Feldhaus and A. Roth, "A 1 MHz to 50 GHz direct down-conversion phase noise analyzer with cross-correlation", in *2016 European Frequency and Time Forum (EFTF)*, 2016, pp. 1–4. doi:10.1109/EFTF.2016.7477759

[9] Raspberry Pi Zero, https://www.raspberrypi.com/products/raspberry-pi-zero/

[10] *Overview of 1-wire technology and its use*, Maxim Integrated, 2008. https://www.analog.com/en/resources/technical-articles/guide-to-1wire-communication.html

[11] M. Killenberg *et al.*, "Abstracted Hardware and Middleware Access in Control Applications", in *Proc. ICALEPCS'17*, Barcelona, Spain, Oct. 2017, pp. 840–845. doi:10.18429/JACoW-ICALEPCS2017-TUPHA178

[12] G. Varghese *et al.*, "ChimeraTK - A Software Tool Kit for Control Applications", in *Proc. IPAC'17*, Copenhagen, Denmark, May 2017, pp. 1798–1801. doi:10.18429/JACoW-IPAC2017-TUPIK049

[13] *OPC Unified Architecture*, The OPC Foundation. http://opcfoundation.org/opc-ua/

[14] R. Steinbrück *et al.*, "Control System Integration of a MicroTCA.4 Based Digital LLRF Using the ChimeraTK OPC UA Adapter", in *Proc. ICALEPCS'17*, Barcelona, Spain, Oct. 2017, pp. 1811–1814. doi:10.18429/JACoW-ICALEPCS2017-THPHA166

[15] LabView, 2023, https://www.ni.com

[16] InfluxDB, 2025, https://www.influxdata.com/

[17] SIMATIC WinCC SCADA, 2023, https://new.siemens.com/global/en/products/automation/industry-software/automation-software/scada.html

[18] J. Teichert *et al.*, "Free-electron laser operation with a superconducting radio-frequency photoinjector at ELBE", *Nucl. Instrum. Methods Phys. Res. A*, vol. 743, pp. 114–120, 2014. doi:10.1016/j.nima.2014.01.006